eprints@whiterose.ac.uk
https://eprints.whiterose.ac.uk/

Investigation into Fault Tolerant Capability of a Triple Redundant PMA SynRM Drive

Bo Wang, *IEEE Member*, Jiabin Wang, *IEEE Senior member*, Antonio Griffo, *IEEE Member*, Yanwen Shi

Abstract — **Fault tolerant machine drives are being favored in safety critical applications, thus they are being actively investigated. However, most of the solutions address the winding or switch open circuit only, which is insufficient since intra-phase and inter-phase turn short circuits are more likely in the machine drives as a result of insulation degradation, and the consequences are usually catastrophic. Magnets and capacitor may also fail and cause damage during operation. All these faults should be properly addressed in fault tolerant machine drives for safety critical applications. Hence, a triple redundant, 9 phase (3x3phase) permanent magnet assisted synchronous reluctance machine (PMA SynRM) drive is presented by investigating the fault tolerances against various faults. The different fault behaviors are evaluated and the corresponding fault tolerant capabilities are analyzed. The machine fault tolerance is examined on a 35kW prototype drive. Both the analysis and experimental tests demonstrate that the machine drive exhibits excellent fault tolerant capability under most common types of faults, including the intra-phase and inter-phase short circuit, uncontrolled rectification, demagnetization and DC capacitor fault.**

Index Terms—**Fault tolerant machine drive, turn fault, phase fault, uncontrolled rectification, demagnetization and DC capacitor fault.**

I. INTRODUCTION

PERMANENT magnet machine drives are increasingly being used in electrification of transport, such as aerospace and electric traction [1]. Although they bring the merits of high efficiency and good controllability, high reliability is an essential requirement for the safety critical applications [2]. Hence, special measures have been implemented in drives to achieve fault tolerant or fail-safe feature which enhance the reliability/availability and reduces the losses caused by the failures [3].

An integrated fault tolerant machine drive usually requires techniques of advanced machine drive topology, fault detection [4, 5], fault isolation [6] and mitigation action [7] to accommodate the failure which leads to complex implementation. Hence, most of the fault tolerant systems only address open circuit failure in the windings or switches [8] which is not the most common case in the machine drives [9,

10]. In fact, open circuit only accounts for a small percentage of total failures. Whilst short circuit faults in single phase or different phases, named as intra-phase turn fault and inter-phase turn fault, are more likely to happen. It is caused by winding insulation degradation due to combined electrical, thermal and mechanical stresses and chemical contaminations. Since the turn fault usually involves a few turns, excessive fault current will be induced in the short circuited path due to low impedance. The resultant heat gives rise to local hotspot and cause further damage to the machine [11].

PM machines are widely adopted in high performance applications due to high efficiency and high torque density. However, from the point view of fault tolerance, the PM field poses a potential hazard to the machine since it cannot be turned off in case of a fault [12]. The PM field could induce large short circuit current even the drive has been deactivated [13]. Further, if the drive fails when the machine is rotating at high speed, the electromotive force (emf) may be much higher than the DC link voltage and consequently cause uncontrolled rectification via the freewheeling diodes. This may damage the DC link components if the generated power is excessive and cannot be absorbed [14, 15]. On the other hand, the magnets are also subject to the risk of demagnetization in high temperature and in case of a drive failure [16]. The demagnetization leads to torque reduction and increase in machine currents for closed loop controlled drive under the same load condition. The vicious cycle may continue and cause further increase in temperature and demagnetization.

In terms of the drives, the DC link capacitor is also vulnerable to open circuit fault and aging effect [17]. In case of the open circuit fault, higher voltage fluctuation and current ripple could be expected while capacitor aging will result in higher equivalent impedance and lower capacitance which decreases the filtering effect. It causes higher voltage and current distortion and deteriorates the machine drive performance. Other faults, like bearing failure, rotor and shaft breakage are also likely to occur. However, they are usually solved by regular maintenance and replacement [18].

In fact, the various faults as discussed above are more common than the basic open circuit fault and they cause worse damage effects to the machine drive [10, 19, 20]. Though these faults mentioned has been discussed in literature in terms of the fault behavior and detection techniques. However, for safety critical applications, the key is to be able to tolerant these faults so that the drive can continue its operation with appropriate remedial action following fault detection. In this respect, the accommodations of these faults have not been fully addressed and experimentally demonstrated to date.

Bo Wang is with the School of Electrical Engineering, Southeast University, Nanjing, 210096, China (Email: bowang.ee@hotmail.com).

J. Wang, A. Griffo, Y. Shi are with the Department of Electronic and Electrical Engineering, University of Sheffield, Sheffield S3 7HQ, U.K (Email: j.b.wang@sheffield.ac.uk, a.griffo@sheffield.ac.uk, yshi27@sheffield.ac.uk).
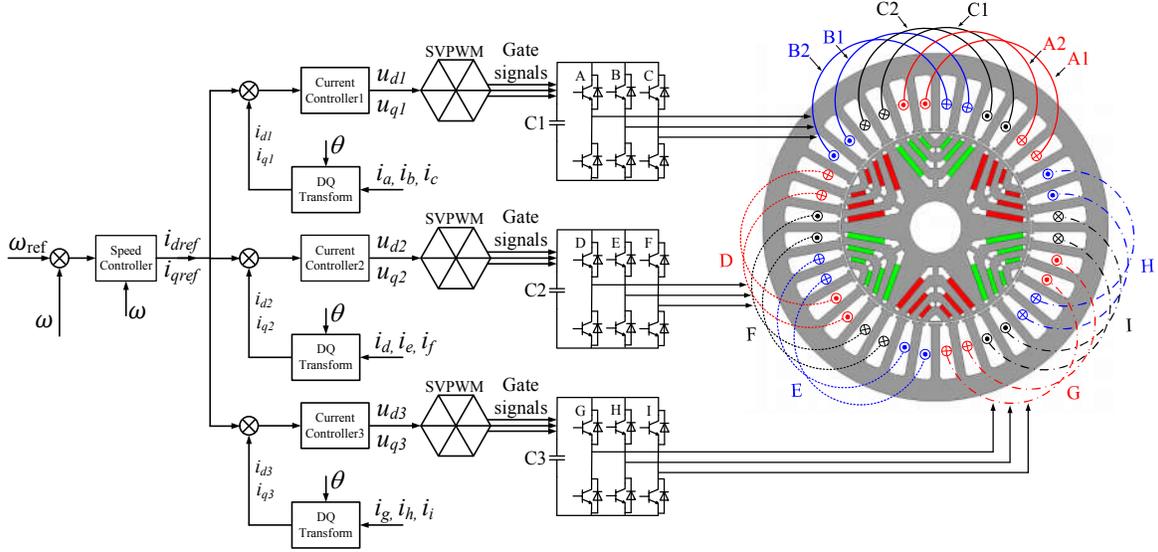
Fig. 1. Triple redundant, 3x3-phase PMA SynRM drive.

Hence, this paper presents a fault tolerant, triple-redundant, 3x3-phase PMA SynRM drive which can accommodate these faults owing to the merits of the employed machine and drive topologies. The intra-phase and inter-phase turn fault, uncontrolled rectification, demagnetization, and DC capacitor fault, etc., all have been investigated in detail regarding the proposed machine drive. The corresponding fault behaviors and fault tolerant capability are analyzed and verified by both FE simulations and experimental tests. In addition, the machine drive can be implemented in a simple and cost-effective manner on the basis of existing widely-used 3-phase IPM drive. Therefore, the proposed machine drive represents a genuine advance in the development of high availability drives for safety critical applications.

II. TRIPLE REDUNDANT 9 PHASE PMA SYNRM DRIVE

The machine under consideration is a 36-slot 6-pole PMA SynRM as shown in Fig. 1 [21]. The machine exhibits comparable performance with conventional PM machines in terms of torque density and efficiency [22]. The high performance is mainly attributed to the hybrid torque production mechanism which combines PM torque and reluctance torque. The reluctance torque enables use of less magnets without sacrificing machine performance. The low PM field reduces fault current in the event of short circuit failure. The resultant low back emf also decreases the possibility of uncontrolled rectification at high speed, therefore improving fault tolerance of the machine drive.

In order to provide further fault tolerance through physical, electrical and thermal isolations, the conventional overlapped distributed windings are divided into three sets of separated 3-phase windings which do not overlap with each other. Three standard 3-phase inverters are employed to drive each 3-phase set, achieving the electrical isolation. The three inverter drive modules share the same speed controller which provides the same current commands for the independent current controllers. Owing to the segregated windings and independent drives, the risk of fault propagation among different 3-phase sets is minimized [23]. Furthermore, any

failure in a single 3-phase set does not significantly affect the operation of other modules. Hence, the remaining healthy sets can continue operation to deliver torque/power.

Table I
SPECIFICATIONS OF THE TRIPLE REDUNDANT PMA SYNRM

Specification	Symbol	Value
Base speed	n_b	4000rpm
Maximum speed	n_m	19200rpm
Rated power	P_r	35kW
Rated current and gamma angle	I_{rated}	120A(51°)
Nominal DC link voltage	V_{dc}	270V
Number of turns per coil	N	8

For this triple redundant fault tolerant machine drive, if open-circuit fault occurs in the inverter switch or windings, the faulty 3-phase winding set can be simply deactivated by opening all the switches in that set. It has been demonstrated in [21] that the machine drive is capable to sustain the open circuit fault with about 1/3 torque reduction. In order to obtain a high availability machine drive, some more severe faults are investigated by FE simulation and experimental test, including the intra-phase and inter-phase turn fault, uncontrolled rectification, demagnetization and DC capacitor fault. The specification of the machine under study is given as in Table I, where the gamma angle refers to the optimal current vector angle with respect to the q-axis for maximum torque per ampere (MTPA) operation.

III. FAULT TOLERANT CAPABILITY INVESTIGATION

In this section, the various faults mentioned above will be analyzed for the triple redundant machine drive using FE simulation. The fault behavior, possible damage and fault tolerant capability are assessed. It is assumed that the detection and classification of the various faults are available [4, 24] but they are not discussed in this paper.

A. Intra-phase Turn Fault

Due to winding insulation break down, short circuit fault may occur in a single phase or between different phases as shown in Fig. 2. It should be noted that the fault can occur at

any position where the insulation has been weaken under combined electrical, thermal and mechanical stress, not necessarily in the end winding region as indicated in Fig. 2. The intra-phase turn fault is reported as the worst fault scenario since only a few turns are short circuited as shown on the left of Fig. 2. The resultant fault current is massive and it decreases with the number of short circuit turns. Thus, the worst case is one turn short circuit located close to slot opening [25].
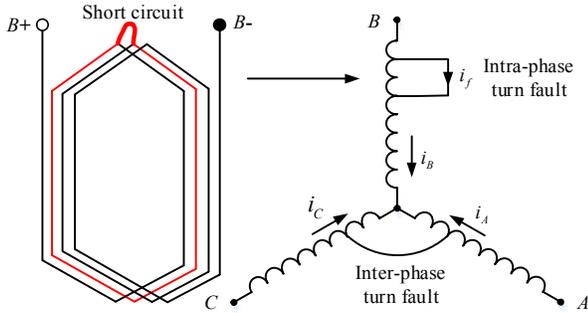

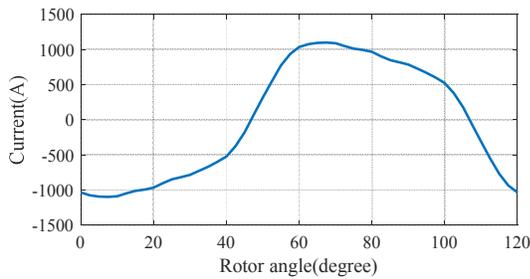Fig. 2. Turn fault illustration.

Fig. 3. Turn fault current in coil B2 with 120A load current at 4000rpm.

Without loss of generality, a single turn fault located in the top of the slot is assumed in coil B2 of set ABC when all the three sets windings are loaded with rated current (120A, 51°) at 4000rpm. The fault is simulated in 2D FE and the resultant fault current i_f reaches 1100A as shown in Fig. 3. This severe fault should be detected and mitigated immediately before developing to a catastrophic failure. Fig. 4(a) shows the flux distribution under the single turn fault condition. Close examination reveals that the flux in coil B2 region is reduced by the fault current in the single short-circuited turn when compared with those in the healthy coils E2 and H2.
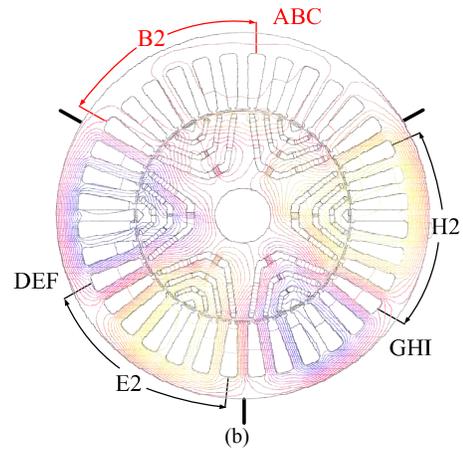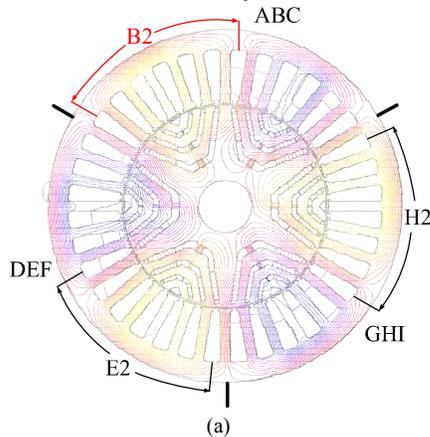

(a)

(b)

Fig. 4. Flux distribution with turn fault in coil B2 (a) without TSC (b) with TSC.

In order to limit the fault current to an acceptable level, terminal short circuit (TSC) can be applied via the inverter of the faulty 3-phase set as mitigation action. Short circuit currents are induced in the healthy turns and coils, and tend to counteract the external flux linkage of the fault set due to the magnets and currents in the healthy sets. Consequently, the residual flux linkage of the fault turn is much lower and the turn fault current is reduced accordingly. The remedy effect of TSC is emulated in FE while the healthy sets are still loaded the same currents (120A, 51°). The turn fault after TSC simulation is performed without co-simulation with inverter drive. Alternatively, current sources are used to represent the inverter drives for two remaining healthy 3-phase sets DEF and GHI under closed-loop current control. Fig. 5 shows the current waveforms in the faulted turn and healthy turns of the ABC set after application of TSC. The phase currents are unbalanced but they are much lower than the rated value due to the low PM flux. Although the turn fault current is 2.6pu, it only involves the single fault turn. Thus, the overall heat effect is lower than the healthy condition which can be thermally contained by the machine as will be examined by experimental test. The flux distribution is shown in Fig. 4(b) where it is evident that the external flux in ABC region is virtually nullified by the short circuit phase currents compared with Fig. 4(a). Hence, the turn fault current is reduced due to lower residual flux. Fig. 6 compares the torque waveforms under the healthy and the fault conditions. Obviously, the machine can still output about 2/3 of healthy torque after the TSC.
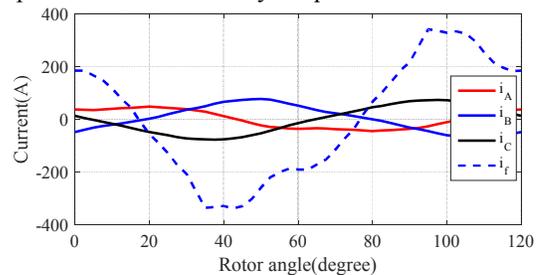

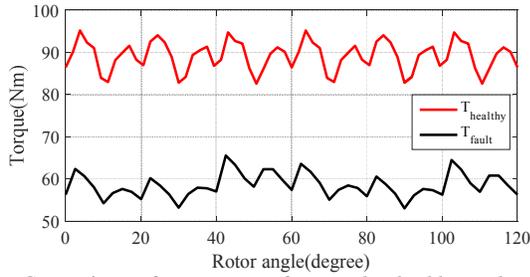Fig. 5. Turn fault current and phase currents in ABC set after TSC.

Fig. 6. Comparison of torque waveform under healthy and turn fault condition after TSC.

Fig. 8. Variations of RMS turn fault currents in 6 coils with load current in healthy 3-phase sets in generating mode.

It should be noted that the short circuited phase currents are quite unbalanced due to the mutual coupling of the healthy sets which are not magnetically isolated. It indicates that the flux linkage of each phase is asymmetrical, which is the combined effect of the magnets, currents in both the fault and healthy sets. Hence, the turn fault current after TSC will be different if it happens in different coil locations as shown in Fig. 1 [21, 26]. And it is influenced by the currents in the healthy sets.

As a result, the turn fault is examined in the 6 different coil locations by varying the currents in the healthy sets under MTPA condition in motoring mode. The variations of RMS fault current after TSC with load currents in the healthy sets at 4000rpm are shown in Fig. 7. It is seen that the fault current is almost always higher if the fault takes place in coil B2, and increases with load current. The reason of the unequal fault current is because after the application of TSC the currents of the three sets are very different, the machine no longer operates in symmetric mode. Hence, the flux linkage of the fault turn is different if it locates in different coils which leads to unequal fault current. And if the currents in the healthy sets vary, the flux linkage of the fault turns also varies, leading to different fault current.

B. Inter-phase Turn Fault

As shown in Fig. 2, if the short circuit fault occurs between different phases, it becomes an inter-phase turn fault. Although the windings of different 3-phase sets are segregated for this machine, the end windings of different phases in the same set are still bundled together. The phase insulation may fail and cause turn fault between phases.

For more clear illustration, the winding of set ABC is shown in Fig. 9. As can be seen, each slot only contains one coil and, therefore, the inter-phase fault may occur in the end winding region. Considering the winding layout, the inter-phase fault is more likely to occur between phases A and C, and between phases B and C as phases A and B do not have any direct contact.

Fig. 9. Winding illustration of set ABC.
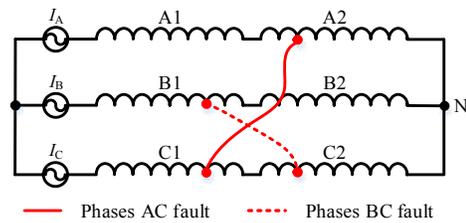
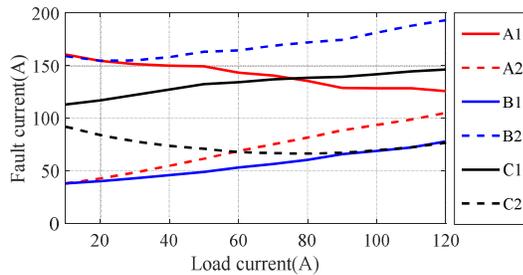Fig. 10. Inter-phase fault illustration.

Fig. 7. Variations of RMS turn fault currents in 6 coils with load current in healthy 3-phase sets in motoring mode.

It should be noted that the maximum turn fault current occurs in coil B2 when the machine is rotating in anti-clockwise direction under motoring mode. However, if the machine is operating in generating mode, the worst turn fault case will occur in coil A1 as shown in Fig. 8. And it is found that the fault current dependency on the coil location exhibits an opposite sequence compared with that of motoring mode. This is because in generating mode, the sequence of the currents in the fault and healthy sets are reversed. Consequently, the flux linkage of the fault turn in coil A1 is the highest and leads to the highest fault current.
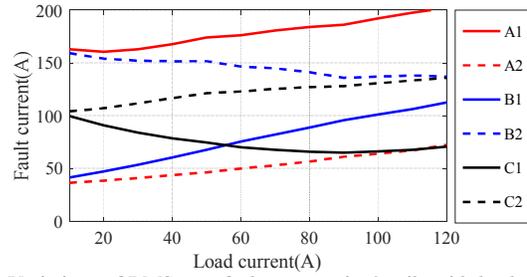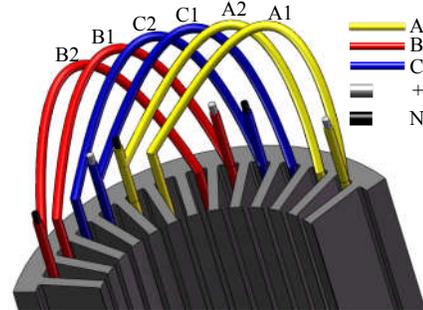
Since coils A2 and C1 are physically overlapped an inter phase fault between these two coils is possible. According to the winding connection in Fig. 10, if there is a short circuit between A2 and C1, coil C2 will be in the short circuit loop. Thus, the number of short circuited turns is always higher than 8, leading to much lower fault current than the intra-phase turn fault. Similar condition is true for short circuit between coils B1 and C2 as shown by the dotted line in Fig. 10. In this case, Coil B2 is included in the short circuit path, resulting in less severe level of fault current.

Although the fault current in inter-phase short circuit is lower than the intra-phase short circuit, TSC still should be applied to the faulted 3-phase set in order to reduce torque pulsation and to avoid excessive local hotspot. It is therefore

necessary to assess the worst case fault current after TSC. The number of short circuited turns may vary depending on the position of short circuit point as shown in Fig. 10. Therefore after application of TSC, 4 extreme inter-phase short circuit cases with the least number of short-circuited turns are shown in Fig. 11. In case 1 to case 4, coils A1, C2, C1 and B2 are effectively short circuited via the neutral or drive supply. Hence the minimum number of short-circuited turns is 8 for the machine under study.
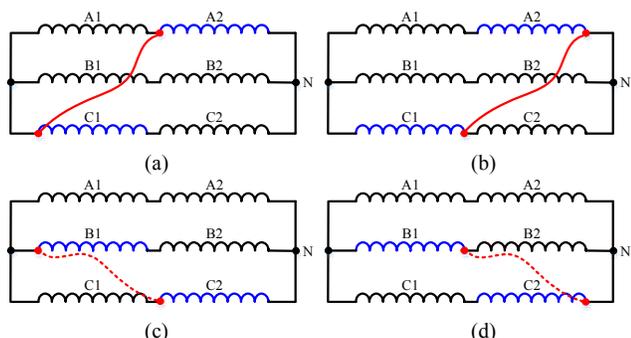

Fig. 11. Extreme inter-phase turn faults (a) case 1 for phases AC fault(b) case 2 for phases AC fault(c) case 3 for phases BC fault(d) case 4 for phases BC fault.

These four extreme inter-phase faults are evaluated when the two healthy 3-phase sets are loaded with rated current at 4000rpm in motoring mode. Again, the highest fault current is observed in case 4 where coil B2 is short circuited. The short circuit currents and resultant torque after TSC are shown in Fig. 12 and Fig. 13. i_{B1} and i_{B2} represent the current in coil B1 and B2, respectively. It is seen that the peak current of i_{B2} is 135A, slightly higher than the rated value. Since other phase currents are much lower, the heat produced by the single coil can be sustained. In addition, the machine can still output 2/3 of healthy torque as shown in Fig. 13.
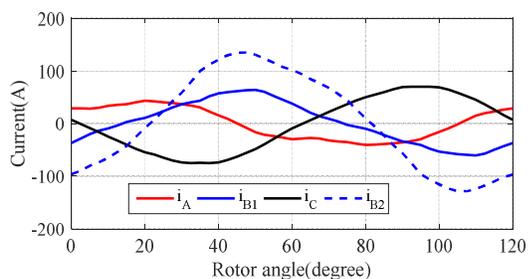

Fig. 12. Short circuit currents for case 4 inter-phase fault.
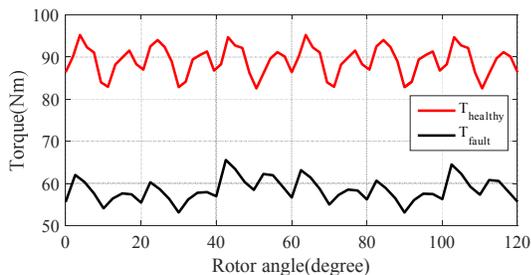

Fig. 13. Torque for case 4 inter-phase fault.

However, if the sequence of coil connections is different from those shown in Fig. 9 and Fig. 10, for example, coils C1 and C2 are swapped, it is quite possible that the last few turns of coils A2 and C1 are short circuited without including another coil in the loop. The resultant fault current will be

much higher. Hence, the winding layout and coil connection should follow Fig. 9 and Fig. 10 to avoid this undesirable condition. Further, insulation paper should be inserted between the phases to enhance the phase-to-phase insulation and reduce the risk of insulation failure.

It should be noted that theoretically two coils may be short-circuited through the stator core even if they do not have direct contact in the end winding region. However, this requires the ground wall insulation breakdown in both coils and hence much less likely.

C. Uncontrolled Rectification Fault

At high speeds, the machine line back emf may be higher than the DC link voltage, especially when a wide constant power operating region (CPOR) is required. This will not be a problem as long as the inverter operates properly in field weakening mode [27]. However, if the inverter fails or applies self-protection due to device overheating or sensing errors, etc., the gate drive signals may be inhibited. The line back emf could be much higher than the DC link voltage and uncontrolled rectifier operation via diodes would take place. Excessive mechanical power is converted to electrical power and flows to the DC link which may damage the whole drives if the regenerated power cannot be absorbed [28].
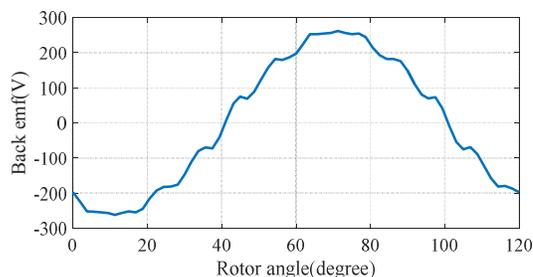

Fig. 14. Line back emf at max speed 19200rpm.
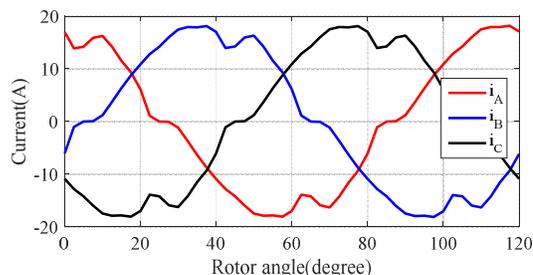
Fig. 15. Phase currents in uncontrolled rectification mode at 23040rpm.

Therefore, the line back emf of the machine has been evaluated at maximum operation speed 19200rpm as shown in Fig. 14. The peak value of the back emf is 262V which is lower than the DC link voltage 270V. The voltage applied on the diodes is always reverse biased. Therefore, the uncontrolled rectification will not occur even if the inverter fails at maximum speed. The machine is designed to have 20% over speed capability beyond which permanent of damage on the rotor will occur. Control measures are usually in place to avoid over speed in most circumstances. Nevertheless, uncontrolled rectifier operation at 120% of the maximum speed 23040rpm in the event of inverter failure is simulated for the prototype drive. Now the line back emf is higher than the DC link voltage and uncontrolled rectification may take place. The resultant phase currents of set ABC are shown in

Fig. 15. It is seen that the phase current is no more than 20A which is safe for the inverter.

This merit is attributed to the combined torque production mechanism of PMA SynRM which enables less use of magnets. The resultant low back emf minimizes the risk of uncontrolled power generation in the event of inverter failure. This fail-safe mode is very desirable for machine drive with a wide CPOR, guaranteeing the safety of high speed operation.

D. Demagnetization Fault

Permanent magnets are vulnerable to demagnetization due to high temperature and excessive armature reaction field under heavy load or fault conditions, like turn fault, terminal short circuit and voltage reversal fault, etc.. It has been identified in [16, 29] that voltage reversal fault is the worst case since the applied voltage U may be out of phase with the back emf E in the event of inverter loss of synchronization. As shown in Fig. 16, these two voltage components combine and produce peak transient current an order of magnitude higher than the rated value, primarily in the negative d-axis direction. Consequently, the magnets will be partially demagnetized.

According to the PM demagnetization BH curve in Fig. 17, if the flux density of any magnet element is lower than the knee point during the fault process, it will operate on the recoil line with reduced remanence in subsequent steps. The machine demagnetization behaviour has been analysed for turn fault, terminal short circuit and voltage reversal fault by repeating the procedures described in [16, 29]. No demagnetisation is found under turn fault, terminal short circuit fault. Partial demagnetization is only observed in the magnets for voltage reversal fault due to the excessive demagnetization currents. The back emf is reduced by 31% compared with the original value. However, the resultant torque is only 9% lower than the rated as shown in Fig. 18. The voltage reversal test will be destructive and unnecessary because the maturity of the modern finite element based simulation tool. Further details of this machine demagnetization can be found in [30].
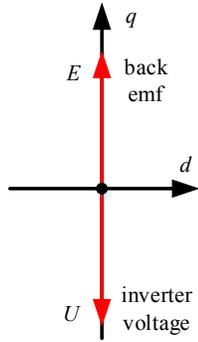

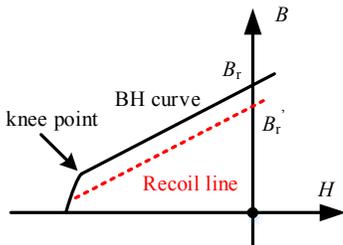Fig. 16. Illustration of inverter loss of synchronization.
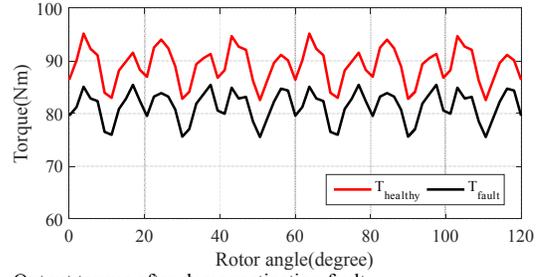

Fig. 17. PM demagnetization BH curve.

Fig. 18. Output torque after demagnetization fault.

As can be seen, although the machine experiences partial demagnetization during the worst fault case, the torque reduction is quite modest. This is because the PM torque only contributes about 30% of the total torque. Thus, the demagnetization fault has a mild impact on the output torque capability. Indeed, it was confirmed in [31] that the PM machine with this type of rotor configuration has the best resistance against demagnetization compared with the surface mounted PM machine, V shape interior PM machine and spoke PM machine.

E. DC Link Capacitor Fault

DC link capacitor is utilized to provide a transient energy buffer and filter out the voltage ripple across the DC link. It is exposed to combined voltage and thermal stress during operation, and hence contributes considerable failure rate in electric drives [32].

Capacitor aging due to electrolyte evaporation and open circuit are the two main failure modes [33]. In case of an open circuit fault, the corresponding inverter should be shut down because of insufficient filtering in the DC link and possible instability of the drive system [34]. The capacitor aging increases the equivalent series resistance and decreases the capacitance. Both effects result in higher current ripple and higher temperature. The inverter also should be turned off to avoid developing to complete breakdown if the capacitor parameters change considerably. Like the open circuit/short circuit fault in the switches and windings, the DC link capacitor failure in one of the 3-phase inverters can also be tolerated by the proposed machine drive with about 2/3 of the healthy torque owing to the triple redundancy.

To tolerate any failure in the DC supply, each 3-phase inverter should be fed by an independent DC source. Hence, loss of DC power in one 3-phase inverter only leads to 1/3 reduction in torque capability.

IV. EXPERIMENTAL TESTS

The fault behavior and fault tolerant capability are tested on a prototype drive whose specification is given in Table I. The machine is mounted on the test rig as shown in Fig. 19 and is connected to the dynamometer via two couplings and an inline torque transducer. The machine is driven in torque control mode by a DSP based 9-phase inverter, consisting of three 3-phase standard inverters as shown in Fig. 20, and loaded by the dynamometer operating in speed control mode. Oil cooling and water cooling are employed for the machine and inverter, respectively. To minimize the tooth ripple effect, the stator has been skewed for one slot angle.
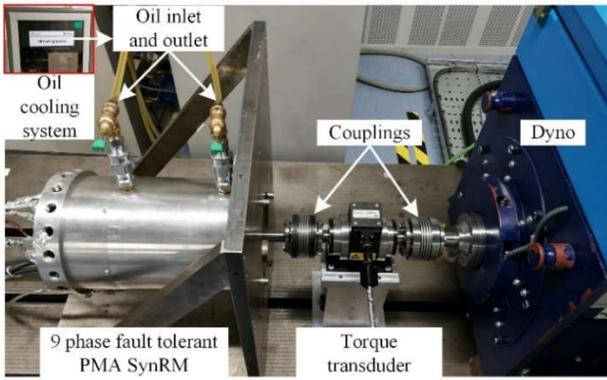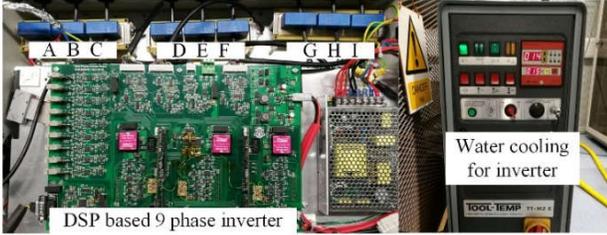
Fig. 19. The 9 phase PMA SynRM test rig.

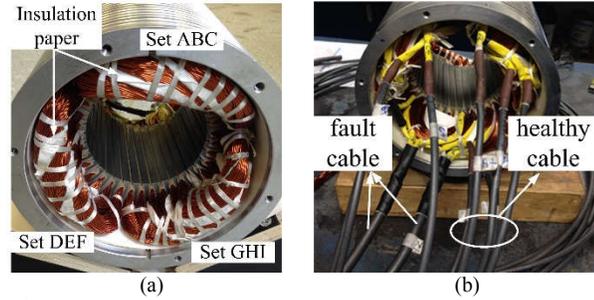Fig. 20. DSP based 9 phase inverter.

(a)   (b)

Fig. 21. End winding and cable leads (a) end winding (b) cable leads.

Fig. 21(a) shows the segregated end windings in which windings of different 3-phase sets do not overlap. To emulate the worst case short circuit condition, a single turn tap is brought out in coil B2 of the ABC windings which is specially positioned close to the top of slot. Thick cables are connected to the fault emulation tap to minimize additional impedance in the short circuited path as shown in Fig. 21(b). The leads is connected with a relay which emulates the intra-phase turn fault. Thermocouples are buried in the slot windings and end winding parts to monitor the thermal behavior under different operation conditions.

A. Back Emf Test

First, the line back emfs of the three 3-phase sets are measured as shown in Fig. 22. The three back emfs of the three sets essentially overlap and match with prediction accounting for the stator skew. This confirms good symmetry between them. Owing to the stator skew, the tooth ripple harmonics in the back emfs are much lower compared with those in Fig. 14. The emfs have been measured over a wide speed range up to 12000rpm and the peak value is shown in Fig. 23. It can be deduced that the peak line-to-line back emf is 246.5V at 19200 rpm, lower than the DC link voltage 270V. Thus, uncontrolled rectification will not occur even if the inverter fails.
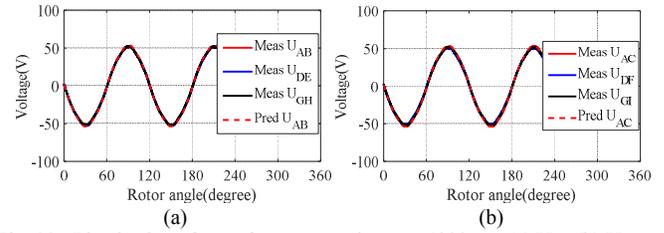

(a)   (b)

Fig. 22. Line back emf waveform comparisons at 4000rpm (a) U_{AB} (b) U_{AC}.
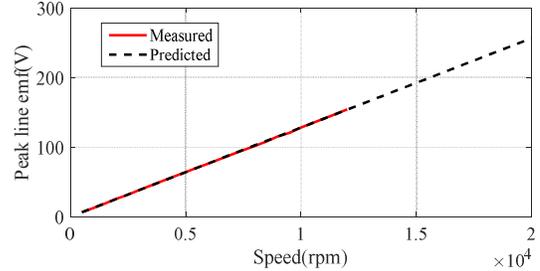

Fig. 23. Variations of peak line back emf with speed.

B. Intra-phase Turn Fault Test

1) Without Terminal Short Circuit

First, the intra-phase short circuit fault without TSC is emulated in coil B2 by closing the relay for 0.3s. Since the fault current would be excessively large at the rated operation point, the fault is emulated at 1000rpm when all three 3-phase sets are excited with 80A under the MTPA condition. The resultant turn fault current is plotted in Fig. 24(a). However, the fault is injected at 0.06s and removed at 0.36s. The current waveforms from 0.05s to 0.15s are shown for clear illustration. It is seen that peak value is 440A which is about 3.7pu. The *dq* axes currents of the three sets are shown in Fig. 25(a). Small disturbance is observed in the first set where the fault occurs while the other two healthy sets currents are almost unaffected.

When the direction of rotor rotation is changed from anti-clockwise to clockwise, the fault turn in coil B2 becomes equivalent to that in coil A1 as shown in Fig. 1. Hence the turn fault in coil A1 is tested by rotating the machine clockwise. The resultant fault current is shown in Fig. 24(b) whose amplitude is similar to that of coil B2 case. The *dq* axes currents are also similar as shown in Fig. 25(b).

Thus, the turn fault current without TSC does not have much difference if it occurs in different coils. This is because the currents of the three sets are still well controlled as shown in Fig. 25. So the flux linkage of the fault turn will be similar if it occurs in different coils. It should be noted that in both cases, the fault currents are excessive, they should be detected and mitigated immediately in real operation.
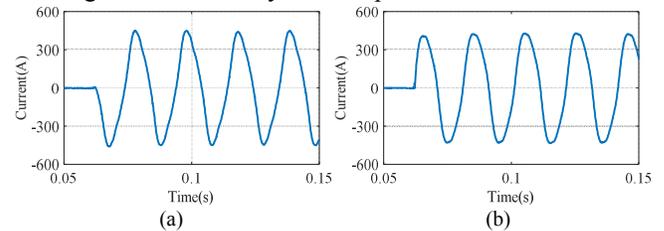

(a)   (b)

Fig. 24. Turn fault current with 80A load current at 1000rpm in motoring mode (a) turn fault in coil B2 (b) turn fault in coil A1.

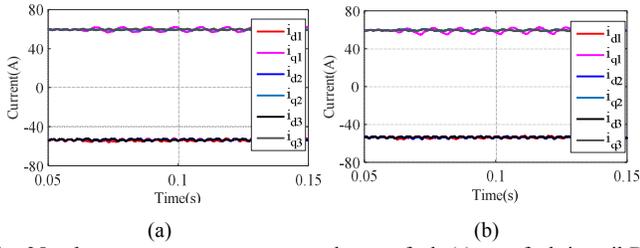(a)   (b)

Fig. 25. *dq* axes currents responses to the turn fault (a) turn fault in coil B2 (b) turn fault in coil A1.

2) With Terminal Short Circuit

Application of TSC can effectively reduce turn fault current. Since the fault current is reduced to a much lower value after TSC, the test can be performed with 120A in healthy 3-phase sets at 4000rpm. For the convenience of testing, TSC is applied to set ABC by manually setting the PWM reference voltage to zero in the DSP controller. First, the turn fault is tested in coil B2. The resultant fault current and phase currents are plotted in Fig. 26(a). It is evident that the fault current is lower than the prediction in Fig. 5 due to additional impedance of the cable leads and relay. The RMS value of the fault current is 1.5pu while the phase current under TSC is much lower than 1.0pu. The currents in the healthy sets are shown in Fig. 27(a). They are still well controlled with small distortion so that the machine drive continues its operation and provides torque. Then, the fault is also tested in coil A1 under the same condition by rotating clockwise. The currents responses are shown in Fig. 26(b) and Fig. 27(a). As can be seen, the fault current is only about 1pu whilst the phase currents are almost the same that of coil B2 case. It confirms that due to the asymmetric currents, the fault current is unequal in different coil locations.

In addition, the turn fault after TSC has been tested in a wide range by varying the load current from 20A to 120A in MTPA condition in both motoring and generating modes. The RMS fault current variations with load currents in healthy sets are measured and plotted in Fig. 28. It is seen that in motoring mode the turn fault current in coil B2 is higher than that in coil A1 while in generating mode the opposite is true. These results are consistent with the predictions in Fig. 7 and the trends are very close. And the post fault torque variation with the excitation currents has been measured and compared with the torque in healthy operation in Fig. 29. It is seen that the machine drive can output about 2/3 of the torque in healthy condition.

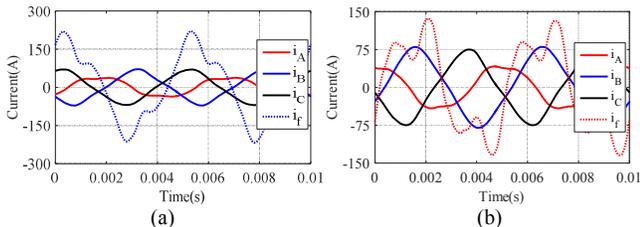(a)   (b)

Fig. 26. Turn fault current and phase currents with 120A load current in motoring mode at 4000rpm after TSC (a) turn fault in coil B2 (b) turn fault in coil A1.

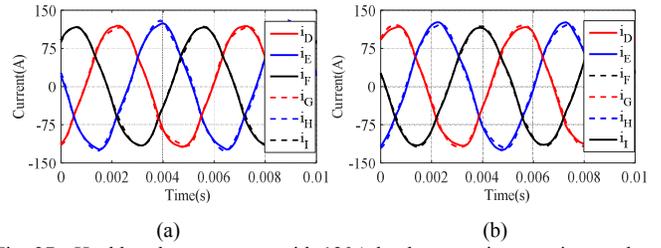(a)   (b)

Fig. 27. Healthy phase currents with 120A load current in motoring mode at 4000rpm after TSC (a) turn fault in coil B2 (b) turn fault in coil A1.
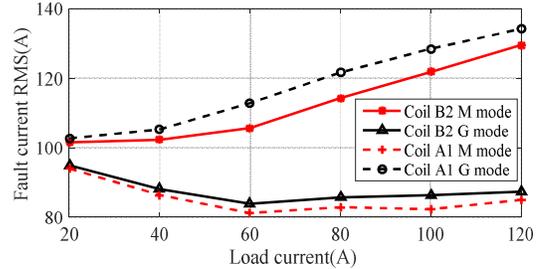

Fig. 28. Variations of RMS turn fault currents with turn fault in coil B2 and A1 at 4000rpm in motoring and generating mode after TSC.
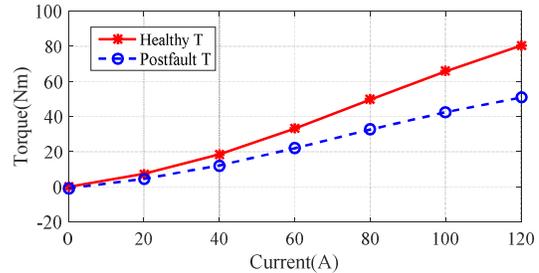
Fig. 29. Variations of the post fault torque with turn fault in coil B2 at 4000rpm in motoring mode after TSC.

To demonstrate the ability of the proposed drive to tolerate the worst turn fault, thermal test is performed for 2 hours when the drive operates at 4000rpm with 120A load current in motoring mode under single turn short circuit in coil B2 with TSC. Fig. 30 shows temperature variations of the oil inlet, outlet, and various parts of the windings when the ambient temperature is controlled as 20°C. It is observed that the temperatures in the slot and end winding where the faulted turn is located are lower than those in the DEF windings though the fault current is 1.5pu. The temperatures of coil B1 and ABC end winding are also lower than that of DEF. This is because the short circuit phase currents are much lower than 120A as shown in Fig. 26. The overall heat is less than the healthy sets. This implies that the machine can operate continuously without overheating after the turn fault with the mitigation action.

Fig. 30. Temperature measurements for turn fault in coil B2 with 120A at 4000rpm in motoring mode after TSC.

The inter-phase turn fault is not tested since it is less severe

than the single turn intra-phase fault. The winding connection has followed those shown in Fig. 10 to avoid undesirable inter-phase fault and insulation paper has been inserted between th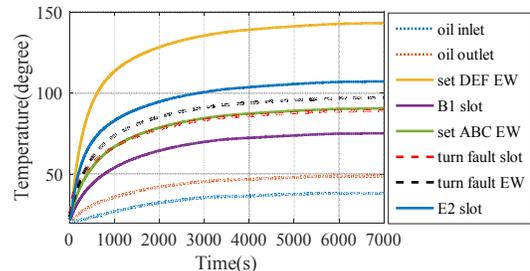e end windings to enhance the phase insulation. The DC capacitor failure in one 3-phase inverter is equivalent to one set open circuit fault whose post-fault operation has been demonstrated in [35]. Therefore, it is also not tested. The fault can be sustained by the triple redundant machine drive with appropriate capacitor condition monitoring technique in place.

V. CONCLUSION

In this paper, the fault tolerant capability of a triple redundant 3x3-phase PMA SynRM drive has been investigated against various types of fault, including intra-phase and inter-phase turn fault, uncontrolled rectification, demagnetization and DC capacitor fault. The fault behaviors and their fault tolerances have been analyzed in detail by extensive FE simulation and experimental tests. It is demonstrated that all these common faults can be accommodated by this single machine drive. Further, implementation of the proposed machine drive is simple and cost-effective. Hence, this machine drive is an ideal candidate for safety critical applications.

REFERENCES

[1] W. Cao, B. C. Mecrow, G. J. Atkinson, J. W. Bennett, and D. J. Atkinson, "Overview of Electric Motor Technologies Used for More Electric Aircraft (MEA)," *Industrial Electronics, IEEE Transactions on,* vol. 59, pp. 3523-3531, 2012.

[2] A. Mohammadpour, S. Mishra, and L. Parsa, "Fault-Tolerant Operation of Multiphase Permanent-Magnet Machines Using Iterative Learning Control," *IEEE Journal of Emerging and Selected Topics in Power Electronics,* vol. 2, pp. 201-211, 2014.

[3] R. V. White, "Fault tolerance in distributed power systems," in *Power Electronics Congress, 1995. Technical Proceedings. CIEP 95., IV IEEE International,* 1995, pp. 121-128.

[4] A. Gandhi, T. Corrigan, and L. Parsa, "Recent Advances in Modeling and Online Detection of Stator Interturn Faults in Electrical Motors," *Industrial Electronics, IEEE Transactions on,* vol. 58, pp. 1564-1575, 2011.

[5] S. Cheng and T. G. Habetler, "Using Only the DC Current Information to Detect Stator Turn Faults in Automotive Claw-Pole Generators," *Industrial Electronics, IEEE Transactions on,* vol. 60, pp. 3462-3471, 2013.

[6] J. W. Bennett, B. C. Mecrow, D. J. Atkinson, and G. J. Atkinson, "Safety-critical design of electromechanical actuation systems in commercial aircraft," *Electric Power Applications, IET,* vol. 5, pp. 37-47, 2011.

[7] B. C. Mecrow, A. G. Jack, D. J. Atkinson, S. R. Green, G. J. Atkinson, A. King*, et al.,* "Design and testing of a four-phase fault-tolerant permanent-magnet machine for an engine fuel pump," *Energy Conversion, IEEE Transactions on,* vol. 19, pp. 671-678, 2004.

[8] S. Dwari, L. Parsa, and T. A. Lipo, "Optimum Control of a Five-phase Integrated Modular Permanent Magnet Motor Under Normal and Open-Circuit Fault Conditions," in *Power Electronics Specialists Conference, 2007. PESC 2007. IEEE,* 2007, pp. 1639-1644.

[9] Y. Song and B. Wang, "Survey on Reliability of Power Electronic Systems," *Power Electronics, IEEE Transactions on,* vol. 28, pp. 591-604, 2013.

[10] A. H. Bonnett and G. C. Soukup, "Cause and analysis of stator and rotor failures in three-phase squirrel-cage induction motors," *Industry Applications, IEEE Transactions on,* vol. 28, pp. 921-937, 1992.

[11] P. Arumugam, "Design Optimization on Conductor Placement in the Slot of Permanent Magnet Machines to Restrict Turn-turn Short-Circuit Fault Current," *IEEE Transactions on Magnetics,* vol. 52, pp. 1-8, 2016.

[12] A. M. El-Refaie, "Fault-tolerant permanent magnet machines: a review," *IET Electric Power Applications,* vol. 5, pp. 59-74, 2011.

[13] J. G. Cintron-Rivera, S. N. Foste, and E. G. Strangas, "Mitigation of Turn-to-Turn Faults in Fault Tolerant Permanent Magnet Synchronous Motors," *IEEE Transactions on Energy Conversion,* vol. 30, pp. 465-475, 2015.

[14] N. Bianchi, S. Bolognani, and M. Zigliotto, "Analysis of PM synchronous motor drive failures during flux weakening operation," in *Power Electronics Specialists Conference, 1996. PESC '96 Record., 27th Annual IEEE,* 1996, pp. 1542-1548 vol.2.

[15] A. M. E.-. Refaie, M. R. Shah, and K. K. Huh, "High-Power-Density Fault-Tolerant PM Generator for Safety-Critical Applications," *IEEE Transactions on Industry Applications,* vol. 50, pp. 1717-1728, 2014.

[16] V. I. Patel, J. Wang, and S. S. Nair, "Demagnetization Assessment of Fractional-Slot and Distributed Wound 6-Phase Permanent Magnet Machines," *Magnetics, IEEE Transactions on,* vol. 51, pp. 1-11, 2015.

[17] C. Peng and A. Q. Huang, "A protection scheme against DC faults VSC based DC systems with bus capacitors," in *2014 IEEE Applied Power Electronics Conference and Exposition - APEC 2014,* 2014, pp. 3423-3428.

[18] "Report of Large Motor Reliability Survey of Industrial and Commercial Installations, Part I," *Industry Applications, IEEE Transactions on,* vol. IA-21, pp. 853-864, 1985.

[19] B. Sen and J. Wang, "Stator Interturn Fault Detection in Permanent-Magnet Machines Using PWM Ripple Current Measurement," *IEEE Transactions on Industrial Electronics,* vol. 63, pp. 3148-3157, 2016.

[20] J. Zhang, J. Hang, S. Ding, and M. Cheng, "Online Diagnosis and Localization of High-Resistance Connection in PMSM With Improved Fault Indicator," *IEEE Transactions on Power Electronics,* vol. 32, pp. 3585-3594, 2017.

[21] B. Wang, J. Wang, and A. Griffo, "A Fault Tolerant Machine Drive Based on Permanent Magnet Assisted Synchronous Reluctance Machine " in *Energy Conversion Congress and Exposition (ECCE), 2016 IEEE,* Milwaukee, WI, 2016, pp. 1-8.

[22] P. Guglielmi, N. G. Giraudo, G. M. Pellegrino, and A. Vagati, "P.M. assisted synchronous reluctance drive for minimal hybrid application," in *Industry Applications Conference, 2004. 39th IAS Annual Meeting. Conference Record of the 2004 IEEE,* 2004, pp. 1-306.

[23] O. V. Thorsen and M. Dalva, "A survey of faults on induction motors in offshore oil industry, petrochemical industry, gas terminals and oil refineries," in *Petroleum and Chemical Industry Conference, 1994. Record of Conference Papers., Institute of Electrical and Electronics Engineers Incorporated Industry Applications Society 41st Annual,* 1994, pp. 1-9.

[24] S. Nandi, H. A. Toliyat, and X. Li, "Condition monitoring and fault diagnosis of electrical motors-a review," *IEEE Transactions on Energy Conversion,* vol. 20, pp. 719-729, 2005.

[25] B. Sen and J. Wang, "Analytical modelling of stator turn fault in surface mounted permanent magnet machines," in *Energy Conversion Congress and Exposition (ECCE), 2013 IEEE,* 2013, pp. 4445-4452.

[26] D. C. Patel and M. C. Chandorkar, "Modeling and Analysis of Stator Interturn Fault Location Effects on Induction Machines," *IEEE Transactions on Industrial Electronics,* vol. 61, pp. 4552-4564, 2014.

[27] T. M. Jahns and V. Caliskan, "Uncontrolled generator operation of interior PM synchronous machines following high-speed inverter shutdown," *IEEE Transactions on Industry Applications,* vol. 35, pp. 1347-1357, 1999.

[28] L. Chong-Zhi, W. L. Soong, B. A. Welchko, and N. Ertugrul, "Uncontrolled generation in interior permanent-magnet Machines," *IEEE Transactions on Industry Applications,* vol. 41, pp. 945-954, 2005.

[29] S. S. Nair, V. I. Patel, and J. Wang, "Post-Demagnetization Performance Assessment for Interior Permanent Magnet AC Machines," *IEEE Transactions on Magnetics,* vol. 52, pp. 1-10, 2016.

[30] Y. Shi and J. Wang, "Continuous demagnetization assessment for triple redundant 9-phase fault-tolerant permanent magnet machine," in *Power Electronics, Machines and Drives (PEMD 2018), 9th IET International Conference on,* 2018, pp. 1-6.

[31] A. Fasolo, L. Alberti, and N. Bianchi, "Performance Comparison Between Switching-Flux and IPM Machines With Rare-Earth and Ferrite PMs," *IEEE Transactions on Industry Applications,* vol. 50, pp. 3708-3716, 2014.

[32] P. Sun, C. Gong, X. Du, Q. Luo, H. Wang, and L. Zhou, "Online Condition Monitoring for Both IGBT Module and DC-Link Capacitor of Power Converter Based on Short-Circuit Current Simultaneously,"

IEEE Transactions on Industrial Electronics, vol. 64, pp. 3662-3671, 2017.

[33] T. Kamel, C. Diduch, Y. Bilestkiy, and L. Chang, "Fault diagnoses for the Dc filters of power electronic converters," in *2012 IEEE Energy Conversion Congress and Exposition (ECCE)*, 2012, pp. 2135-2141.

[34] J. Wang and D. Howe, "A Power Shaping Stabilizing Control Strategy for DC Power Systems With Constant Power Loads," *IEEE Transactions on Power Electronics,* vol. 23, pp. 2982-2989, 2008.

[35] B. Wang, J. Wang, B. Sen, and A. Griffo, "A Fault Tolerant Machine Drive Based on Permanent Magnet Assisted Synchronous Reluctance Machine," *IEEE Transactions on Industry Applications,* vol. early access, pp. 1-8, 2018.

Bo Wang (M'17) received the B.Eng. and M.Sc. degrees in electrical engineering from Nanjing University of Aeronautics and Astronautics, Nanjing, China, in 2009 and 2012, respectively and the Ph.D. degree in Electronic and Electrical Engineering from the University of Sheffield, Sheffield, U.K., in 2018.

From 2012 to 2014, he served as a senior engineer in the Delta Electronics Co. Ltd. From 2017 to 2018, he was a research associate at the Department of Electronic and Electrical Engineering, University of Sheffield. His research interests include the permanent magnet machine drives, electric traction and fault tolerant systems.

Antonio Griffo (M'13) received the M.Sc. degree in electronic engineering and the Ph.D. degree in electrical engineering from the University of Napoli "Federico II," Naples, Italy, in 2003 and 2007, respectively. From 2007 to 2013, he was a Research Associate with the University of Sheffield, Sheffield, U.K., and the University of Bristol, Bristol, U.K. He is currently a Lecturer with the Department of Electronic and Electrical Engineering, University of Sheffield. His research interests include modeling, control and condition monitoring of electric power systems, power electronics converters, and electrical motor drives, for renewable energy, automotive and aerospace applications.

Jiabin Wang (SM'03) received the B.Eng. and M.Eng. degrees from Jiangsu University, Zhengjiang, China, in 1982 and 1986, respectively, and the Ph.D. degree from the University of East London, London, U.K., in 1996, all in electrical and electronic engineering.

Currently, he is a Professor in Electrical Engineering at the University of Sheffield, Sheffield, U.K. From 1986 to 1991, he was with the Department of Electrical Engineering at Jiangsu University, where he was appointed a Lecturer in 1987 and an Associated Professor in 1990. He was a Postdoctoral Research Associate at the University of Sheffield, Sheffield, U.K., from 1996 to 1997, and a Senior Lecturer at the University of East London from 1998 to 2001. His research interests range from motion control and electromechanical energy conversion to electric drives for applications in automotive, renewable energy, household appliances and aerospace sectors.

He is a fellow of the IET and a senior member of IEEE.

Yanwen Shi was born in Jiangsu, China, in 1991. She received the B.Eng. and M.Eng. degrees in electrical engineering from Harbin Institute of Technology , Harbin, China, in 2013 and 2015, respectively. Currently, she is working toward the Ph.D. degree in electronic and electrical engineering, University of Sheffield, Sheffield, U.K.

Her research interests include the modeling, design, and analysis of permanent-magnet synchronous machines for safety-critical applications.